

**Titre:** Microstructural and fatigue characterization of 316L stainless steel subjected to flow drilling and tapping: comparison with machined threads  
**Title:**

**Auteurs:** Mohamed Akram Mechter, Mina Gadour, Léa Romain, Oguzhan Tuysuz, & Myriam Brochu  
**Authors:**

**Date:** 2024

**Type:** Article de revue / Article


**Référence:** Mechter, M. A., Gadour, M., Romain, L., Tuysuz, O., & Brochu, M. (2024). Microstructural and fatigue characterization of 316L stainless steel subjected to flow drilling and tapping: comparison with machined threads. Engineering Failure Analysis, 164, 108730 (13 pages).  
**Citation:**  
<https://doi.org/10.1016/j.engfailanal.2024.108730>

 **Document en libre accès dans PolyPublie**  
Open Access document in PolyPublie

**URL de PolyPublie:** <https://publications.polymtl.ca/59026/>  
**PolyPublie URL:**

**Version:** Version officielle de l'éditeur / Published version  
Révisé par les pairs / Refereed

**Conditions d'utilisation:** CC BY-NC  
**Terms of Use:**

 **Document publié chez l'éditeur officiel**  
Document issued by the official publisher

**Titre de la revue:** Engineering Failure Analysis (vol. 164)  
**Journal Title:**

**Maison d'édition:** Elsevier  
**Publisher:**

**URL officiel:** <https://doi.org/10.1016/j.engfailanal.2024.108730>  
**Official URL:**

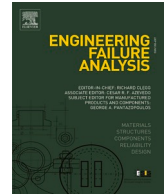
**Mention légale:**  
**Legal notice:**



ELSEVIER

Contents lists available at ScienceDirect

# Engineering Failure Analysis

journal homepage: [www.elsevier.com/locate/engfailanal](http://www.elsevier.com/locate/engfailanal)

## Microstructural and fatigue characterization of 316L stainless steel subjected to flow drilling and tapping: comparison with machined threads

Mohamed Akram Mechter<sup>\*</sup>, Mina Gadour, Léa Romain, Oguzhan Tuysuz, Myriam Brochu

Polytechnique Montreal, 2500 Chem. de Polytechnique, Montréal, QC H3T 1J4, Canada

### ARTICLE INFO

#### Keywords:

Locking compression plate  
316L Stainless steel  
Failure analysis  
Mechanical testing  
Fatigue  
Manufacturing defect

### ABSTRACT

Despite extensive research on the plastic deformation of materials to enhance their fatigue resistance, the influence of the flow tapping process on the fatigue resistance of drilled and tapped bars remains poorly understood. Herein, the fatigue performance of flow-drilled (friction-drilled) and flow-tapped 316L stainless steel bars was experimentally analyzed and compared with that of conventional material-shearing-based drilling and tapping operations. The effect of flow processes on the material properties was evaluated via microhardness tests and microstructural analyses. The results indicated that the hardness near the holes produced via flow forming was 62 % higher than that of the base metal. Moreover, grain refinement and plastic deformation were observed beneath the thread surfaces. Metallographic observations revealed the occurrence of craters and folds at the crest of the flow-formed threads. Following the ASTM F382-17 standard, four-point bending fatigue tests were performed at three stress amplitudes with a stress ratio of 0.1. No noteworthy differences were observed when the maximum bending moments applied were at 75 % and 60 % of the bending moment at yield. However, when the maximum bending moment applied was limited to 50 % of the bending moment at yield, the average fatigue life of the specimens with machined threads was longer than that of their flow-formed counterparts. Fractographic observations were used to identify the crack initiation regions and elucidate the underlying fracture mechanisms. For both types of specimens, failure originated at the crest of the first thread, beneath the surface of the maximum tensile stress. The flow-processed specimens exhibited secondary cracks at the root of the threads, where grain refinement also occurred. This study provides robust empirical evidence that using flow-forming processes to thread 316L stainless steel does not systematically improve the fatigue resistance of the material surrounding the holes. Furthermore, by optimizing the flow process and eliminating discontinuities, the threading process proposed herein could help improve the fatigue resistance of orthopedic implants.

### 1. Introduction

Flow drilling is a plastic deformation process used for generating holes via the penetration of a rigid rotating tool into the material

<sup>\*</sup> Corresponding author at: Polytechnique Montreal, 2500 Chem. de Polytechnique, Montréal, QC H3T 1J4, Canada.  
E-mail address: [mohamed-akram.mechter@polymtl.ca](mailto:mohamed-akram.mechter@polymtl.ca) (M.A. Mechter).

<https://doi.org/10.1016/j.engfailanal.2024.108730>

Received 7 May 2024; Received in revised form 11 July 2024; Accepted 31 July 2024

Available online 31 July 2024

1350-6307/© 2024 The Authors. Published by Elsevier Ltd. This is an open access article under the CC BY-NC license (<http://creativecommons.org/licenses/by-nc/4.0/>).

(Fig. 1). The material is heated owing to the friction between the rotating tool and the material (Fig. 1a). Subsequently, an axial force is applied to plastically extrude the material (Fig. 1b and c). Similarly, flow tapping forms threads via the plastic deformation of the bushing created by the flow drilling process. In contrast to the process of shearing the material, threads are formed on the parent material without heating. Notably, both forming processes influence the microstructure and induce local material hardening. The material flow resulting from flow drilling is illustrated in Fig. 1d. The horizontal lines on the material being drilled illustrate the presence of an elongated microstructure before the drilling process, typical of rolled products. During drilling, the material flows in the direction of the force vector to form the lower bushing and in the opposite direction to form the upper bushing containing the displaced material.

Rolling is a manufacturing process used to produce male threads with enhanced fatigue resistance. This process involves plastically deforming the material instead of cutting (shearing) it to form threads. Armentia et al. [1] experimentally demonstrated that cold rolled screws have a nine times longer fatigue life than that of machined screws. They measured a 180 % increase in compressive residual stresses at the surface of rolled threads compared with that of machined threads. Fromentin [2] experimentally measured the residual stress at the surface of threads formed via flow tapping, a plastic deformation process used to form female threads.

Contrary to machining (Fig. 2a), flow tapping creates a specific plastic deformation pattern, as illustrated in Fig. 2b. The plastic deformation pattern depends on the flow process. In this study, the term “flow-processed” is adopted to denote the process of producing a threaded hole via successive flow drilling and flow tapping.

Various researchers have examined the influence of flow processes on material properties. For example, Miller et al. [3,4] investigated the effect of flow drilling on hole surface integrity and highlighted the importance of optimizing the flow drilling conditions to limit surface damage. Chow et al. [5] demonstrated the feasibility of obtaining a hole with a surface roughness of  $0.96 \mu\text{m}$  without any visible surface discontinuities. This surface integrity is superior to that (typical roughness of  $1.6$  to  $6.3 \mu\text{m}$ ) achieved by [6] via drilling with shearing (chip generation).

Additionally, Miller et al. [3] and Chow et al. [5] reported the occurrence of strain hardening and grain refinement at the hole surface during flow drilling. Moreover, Chow et al. [5] reported an increase of up to 40 % in microhardness at the surface of the hole as well as grain refinement at a depth of 3 mm underneath the hole surface. Similar findings [7] have been obtained without any reference to potential surface discontinuities.

Fromentin [2] reported that flow tapping resulted in a nearly 100 % increase in microhardness at the thread root, with grain refinement extending up to  $300 \mu\text{m}$  underneath the root surface.

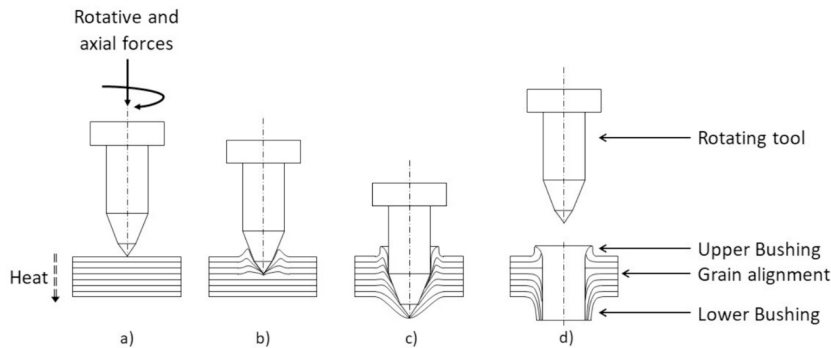


Fig. 1. Flow drilling and material flow during and after the operation. The rectangular part represents a plate with an elongated microstructure.

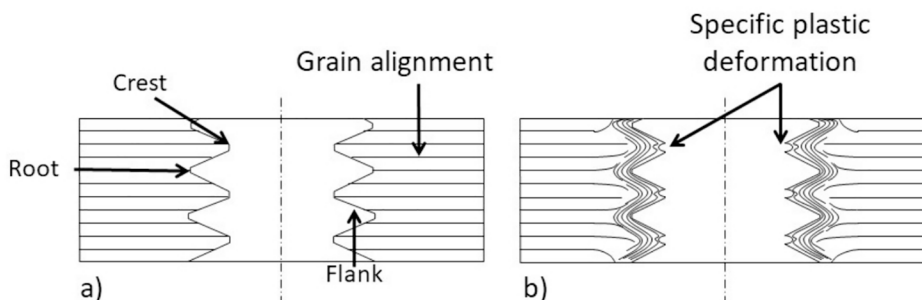


Fig. 2. A) machined threads and b) flow-tapped threads. the horizontal lines on the material illustrate the presence of an elongated microstructure before the drilling and tapping processes.

Considerable experimental research and case studies have demonstrated that fatigue failures often originate from threaded holes. For example, Gervais et al. [8] investigated the premature failure of a broken stainless steel orthopedic implant via fractographic observations and noted that a fatigue crack initiated from the threaded hole. Moreover, Mohajerzadeh et al. [9] and Kanchanomai et al. [10] experimentally observed the occurrence of crack initiation at tapped holes. However, given the limited investigation on the effect of flow forming on the fatigue life, we considered the findings of shot-peening studies linking the influence of local plastic deformation on the fatigue strength of materials. This may be reasonable as shot peening also induces compressive residual stresses, material hardening, and grain refinement via local plastic deformation. Unal et al. [11] demonstrated that shot peening increased the fatigue life of AISI 1050 steel, despite its adverse effect on the surface roughness. They argued that the improvement in fatigue life was attributable to an increase in the microhardness and presence of compressive residual stresses. Similarly, Zhi et al. [12] examined the effects of double shot peening on the fatigue life of an A100 steel plate-hole. They found that under the high cycle fatigue regime, conventional shot peening could enhance fatigue life by only 16.09 %, whereas double peening resulted in a significant improvement of up to 59.60 %. This outcome suggests that the combined effect of the plastic deformation induced by flow drilling and flow tapping could enhance fatigue life.

In summary, local work hardening has proven to be beneficial for fatigue life and, it could improve the fatigue resistance of threaded holes. Although prior studies have explored the effect of flow drilling and flow tapping independently, their combined influence on the fatigue life of metals remains to be comprehensively investigated. Furthermore, despite extensive studies in this domain, the influence of the flow-tapping process on the fatigue resistance of drilled and tapped bars remains unexplored. Thus, this study is aimed at improving the fatigue life of locking compression plates (LCPs) by quantifying the potential of flow-forming processes in mitigating the premature fatigue failures of stainless-steel implants. Specifically, we comprehensively compare and elucidate the fatigue behavior of stainless-steel bars subjected to drilling and tapping as well as flow forming.

The remainder of this paper is organized as follows: First, the experimental methodology is outlined, including sample characterization and fatigue testing. Next, the experimental results are presented, along with a comparative analysis of the specimen microstructures and fractographies. Finally, the concluding remarks are presented, and the scope for future study is highlighted.

## 2. Material and experimental procedure

### 2.1. Material properties

Since flow forming is not yet used to drill and tap holes of biomedical implants, thirty rectangular samples having dimensions comparable to locking compression plates were manufactured from hot rolled 316L stainless steel bars. According to ASTM F-138 this material is commonly used for biomedical plate type implants. Fig. 3 depicts the dimensions of the specimens, and Table 1 summarizes the material properties as given by the manufacturer.

To create holes, drilling, and tapping (C) techniques were used for 15 of the samples, whereas flow drilling and flow tapping (F)

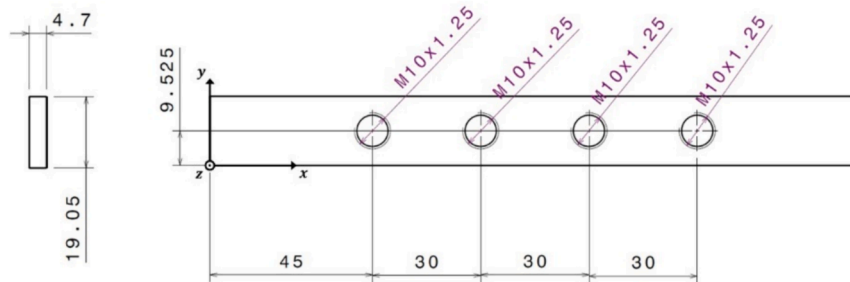


Fig. 3. Dimensions of the fatigue specimens (mm).

Table 1

Material properties, derived from the material certificate provided by the supplier. The chemical composition is presented in weight %.

316L Stainless steel									
C	Mn	P	S	Si	Cr	Ni	Mo	Cu	N2
0.0160	1.3200	0.0400	0.0020	0.1100	16.6300	10.0200	2.0400	0.5000	0.0500
			Yield 329 MPa	Tensile 614 MPa	48 %	HRB 84			

were used for the remaining 15. Table 2 lists the manufacturing conditions.

2.2. Experimental procedures

Microhardness tests and microstructural analyses were performed beneath the threaded surfaces. Four planes were examined for each manufacturing process: two y-z planes (passing through two different holes) and two x-z planes (same holes used for the y-z plane cut). Fig. 4 illustrates the preparation process.

The samples were mounted and polished according to the guidelines of ASTM E3-11 [14]. Microhardness profiles were derived in both the longitudinal and transversal directions according to ASTM E384-22 [15] guidelines. For measurements taken at distances smaller than 500 μm from the surface, a mass of 25 g was used, whereas a mass of 100 g was used for all other regions. The microstructure was revealed by immersing the samples in a solution of Aqua Regia (150 mL distilled water, 50 mL HCl, and 50 mL of HNO<sub>3</sub>) for 40 s to 1 min.

Since the use of the flow process aims to improve the fatigue resistance of plate type implants, fatigue tests were conducted according to ASTM F382-17 guidelines using a four-point bending setup with upper and lower fixture spans of 30 and 120 mm, respectively. The setup and sample are illustrated in Fig. 5. Fatigue tests were conducted using a stress ratio (R) of 0.1 at three stress amplitudes. For both manufacturing processes, five samples were tested at these stress amplitudes, with frequencies ranging from 40 to 45 Hz.

Table 2  
Process parameters and tool specifications.

Manufacturing parameters	Machining		Flow	
	drilling	tapping	drilling	tapping
Feed rate (mm/min)	127	238	260	10
Rotation speed (rpm)	800	200	1900	160
Lubricant	Hangsterfers S-737 at 7–9 %		FDKSO	N/A
Tool material	Carbide		HSS	Carbide
Tool coating	AlTiN PVD	X	N/A	N/A
Tool cone angle (°)	140	X	N/A	X
Tool diameter	8.8 mm	M10 1.25	9.3 mm	M10 1.25

X: if none.  
N/A: if unknown.

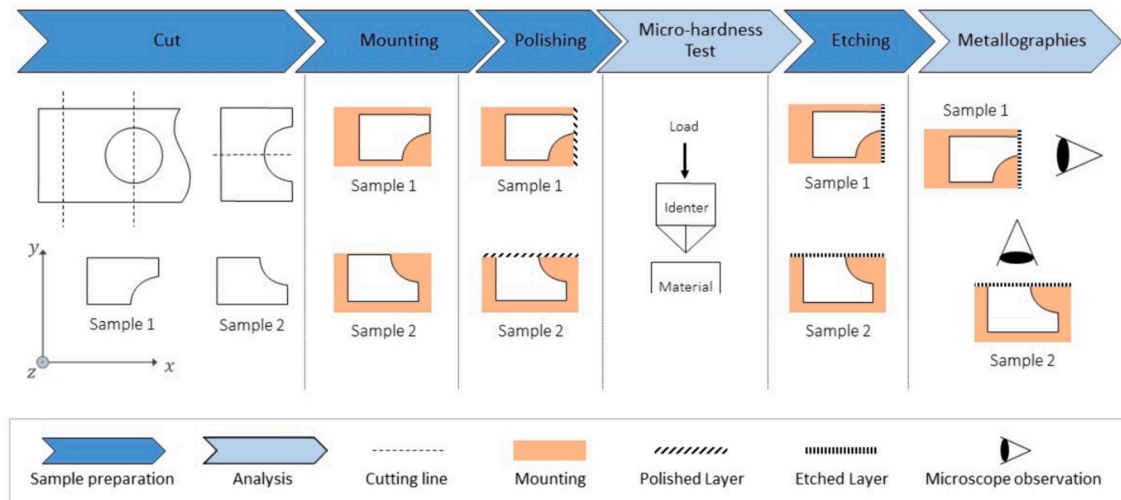


Fig. 4. Preparation and analysis of the examined planes. Samples 1 and 2 pertain to the y-z and x-z planes, respectively.

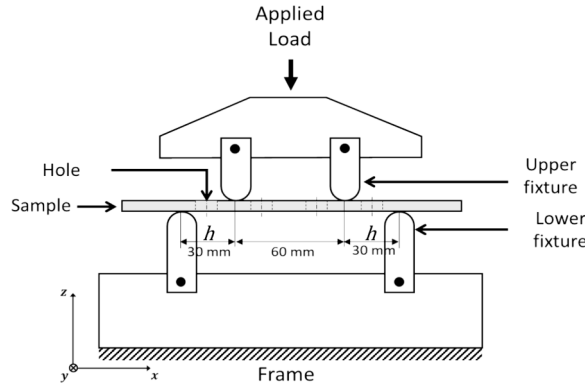


Fig. 5. Four-point bending setup and fatigue sample.

The stress amplitudes were selected such that the maximum force applied,  $F_{max}$ , was 75 %, 60 %, and 50 % of the force required to yield the bar under monotonic bending. This load ( $F_{yield}$ ) was measured in advance.

Table 3 summarizes the fatigue test plan, where  $F$  denotes the force applied in the  $z$  direction by the upper fixture.

### 3. Results and analysis

#### 3.1. Sample characterization

Fig. 6 presents the outcomes of Vickers microhardness evaluations, with the value increasing with decreasing distance from the threaded surfaces. The threads prepared using both manufacturing processes exhibited this trend. For a given process, the results from

Table 3  
Fatigue test conditions for the three load levels.

$F_{max}$ (N) 75 % of $F_{yield}$	$F_{min}$ (N)	Frequency (Hz)
1125	112.5	40
$F_{max}$ (N) 60 % of $F_{yield}$	$F_{min}$ (N)	Frequency (Hz)
950	95	45
$F_{max}$ (N) 50 % of $F_{yield}$	$F_{min}$ (N)	Frequency (Hz)
750	75	45

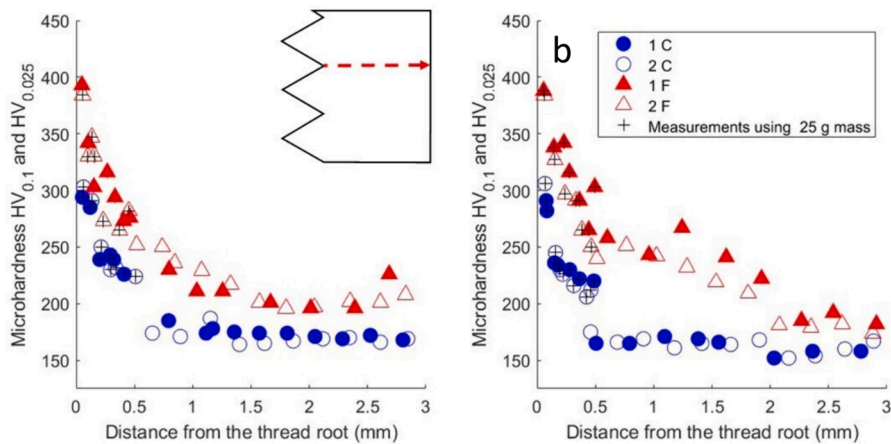
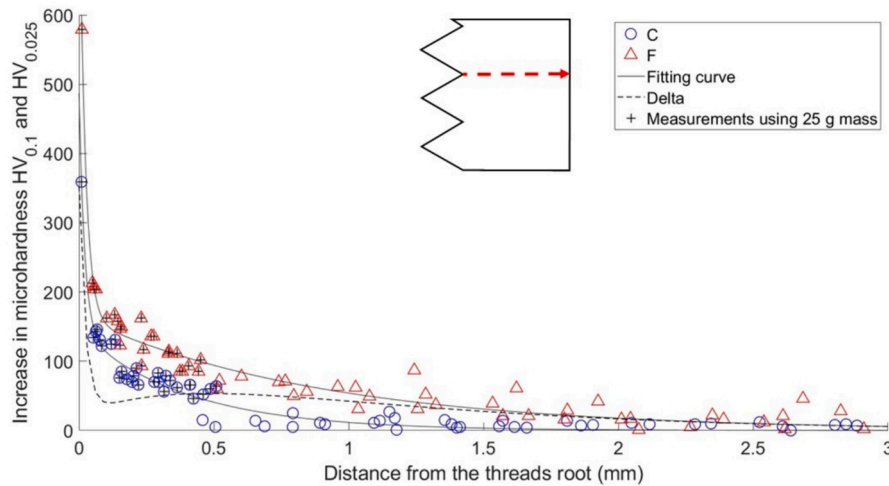


Fig. 6. Vickers microhardness profiles. The 0-distance corresponds to the root of the machined (C) and flow-processed (F) thread samples in the a) x direction and b) y direction.



**Fig. 7.** Increase in Vickers microhardness as a function of the distance from the thread root. The fitted and difference (Delta) curves between machining (C) and flow-processed (F) samples are presented.

the two samples were comparable. A comparison of the hardness profile of the two processes revealed higher microhardness values at all distances for the flow-formed samples.

An analysis of variance was performed to assess the significance of microhardness differences, with the manufacturing process (machining vs. flow processing) being the main factor of analysis. No secondary factors were considered. The obtained  $p$ -value ( $3.472 \times 10^{-9}$ ) was lower than the reference  $p$ -value (0.05), indicating a significant difference in microhardness values for a given distance.

**Fig. 7** shows the difference in microhardness between the local measurements and average bulk material microhardness values. Notably, for a given process, the results of two samples were combined into one dataset owing to their similarity. A bi-exponential equation was fitted to each set of results ( $Cfit(x) = 344.2 \cdot \exp(-48.93 \cdot x) + 142.9 \cdot \exp(-2.51 \cdot x)$  and  $Ffit(x) = 676.3 \cdot \exp(-45.64 \cdot x) + 164.2 \cdot \exp(-1.113 \cdot x)$  with  $Cfit$  and  $Ffit$  for the C and the F sets respectively) to enable interpolation, thereby facilitating a comparative analysis. To identify the distance corresponding to the difference in maximum microhardness between the two processes, a third curve was plotted by subtracting the curve fitting results of machining (C) from those of the flow (F) process. This third curve, identified *Delta*, is presented as a dashed line in **Fig. 7**.

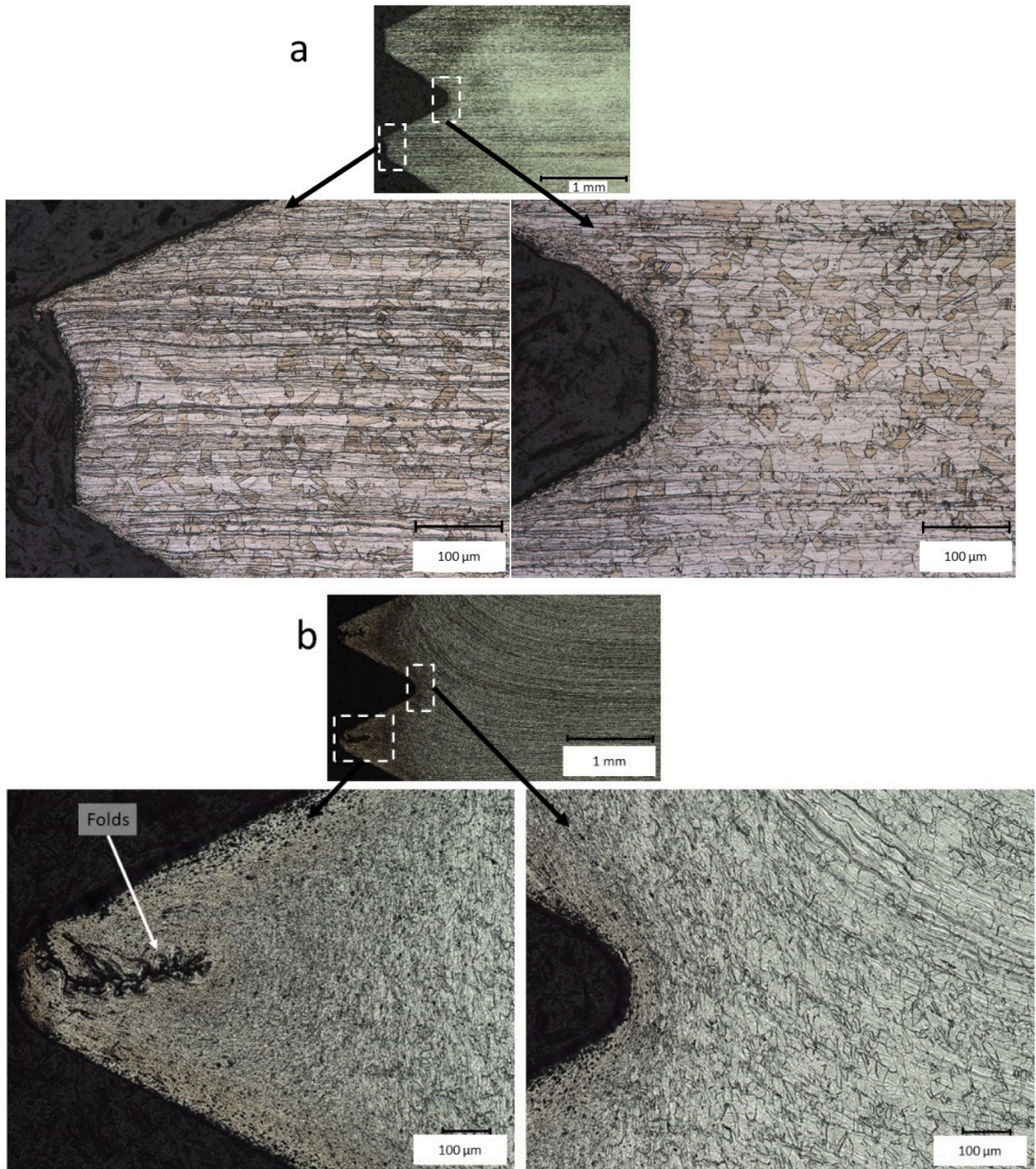
The *Delta* curve clearly indicates a maximum difference of 240 HV at  $10 \mu\text{m}$  beneath the threaded surface. This hardening relative to the bulk material represents a 289 % increase, higher than the value of 40 % reported by Chow et al. [5] and 100 % reported by Fromentin [2]. Unlike the previous studies, which focused on either flow drilling or flow tapping, this study evaluated the combination of both processes, which may account for the differences in findings. Additionally, the results revealed that the hardening depths of the flow forming and machining processes were 2 and 0.5 mm, respectively (**Fig. 7**).

**Fig. 8** shows the metallographic observations of both the C and F samples. In the case shown in **Fig. 8a**, material flow was observed only along the  $x$ -axis, attributable to the rolling process used to shape the bar prior to drilling and tapping. In the cases shown in **Fig. 8b** and 9, the material flowed upward and downward at the thread root. At the crest of the thread, a swirl (or fold) effect was observed. In addition, cracks or craters were observed at the crest of the F threads. According to Fromentin [2], the features at the crest of the thread depend on the forming parameters.

### 3.2. Fatigue tests

According to the ASTM F382-17 standards [16], the results of bending tests should be displayed as bending moment ( $M$ ) – number of cycles ( $N$ ) diagrams. To convert the force applied ( $F$ ) by the loading fixtures into  $M$ , the standard provides the following equation:

$$M = \frac{Fh}{2}$$



*b) Samples and positions of F metallographies*

**Fig. 8.** A) samples and positions of c metallographies b) samples and positions of f metallographies.



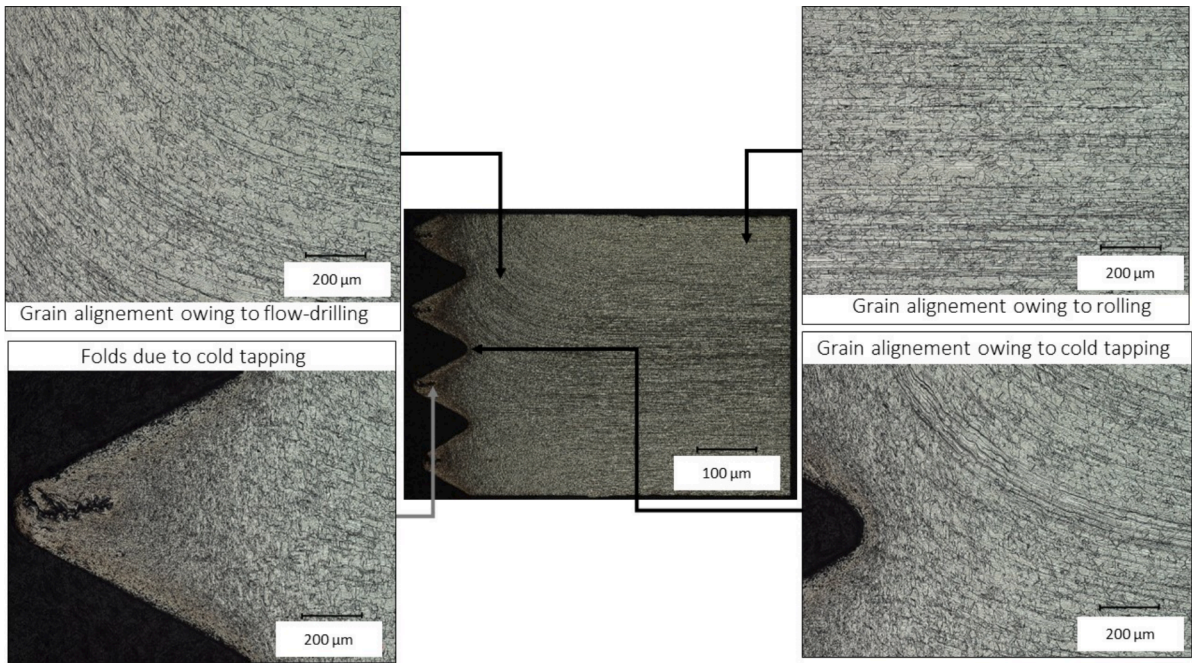


Fig. 9. Metallography of a flow-processed sample.

where  $h$  is the horizontal distance between the lower and upper fixtures. Fig. 10 shows the results of the fatigue tests. No significant differences were observed when the maximum bending moments were 75 % and 60 % of the yield bending moment. Nevertheless, the C specimens outperformed the F samples in terms of fatigue strength when the maximum bending moment was 50 % of the yield bending moment. Specifically, three of the C specimens endured  $10^7$  cycles without failure, whereas five of the F specimens failed before  $10^6$  cycles.

The position and the orientation of the fracture plans are comparable to those observed in real implants as reported in the literature [9,10]. Figs. 11 and 12 present scanning electron microscopy (SEM) observations of typical fractured surfaces of F and C specimens. The images present the ridgelines and beach marks used to identify the crack initiation sites.

For all C specimens, the ridgelines converged toward the crest of the closest thread to the surface under tension. This finding indicated that the crack initiated at the last thread of the entire threaded section.

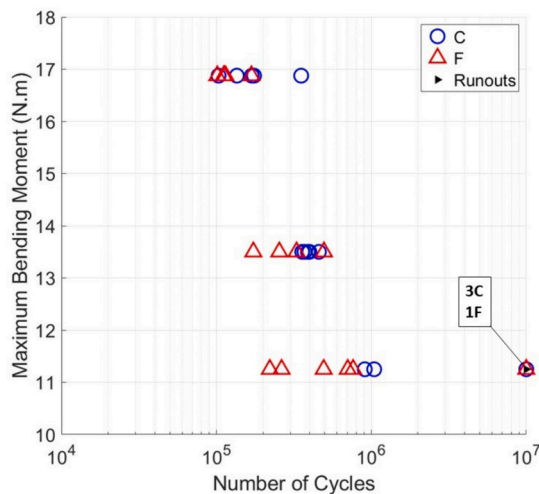


Fig. 10. M–N diagram of machined and flow-processed specimens.

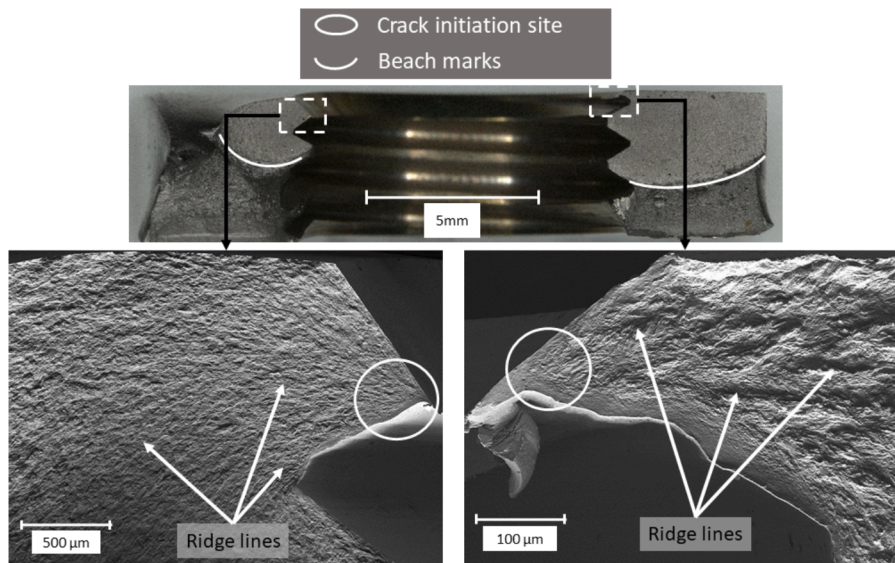


Fig. 11. Fractographies of a C specimen obtained using an optical microscope and scanning electron microscopy (SEM).

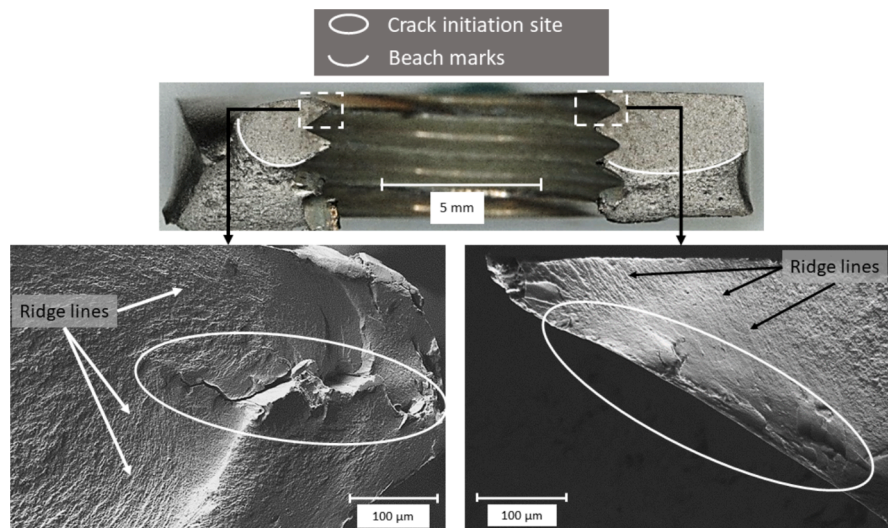


Fig. 12. Fractographies of an F specimen, obtained using an optical microscope and scanning electron microscopy (SEM).

In contrast, for all F specimens, at least one crack was initiated at the crest of a thread within the highly deformed layer. When failure originated from the crest of a thread, the ridgelines converged toward a crack or crater, as shown in Fig. 9. Cracks in other highly deformed regions were also observed (Fig. 13). Flow forming created discontinuities and excessive work hardening, which led to premature crack initiation. This crack initiation mechanism is specific to the flow formed specimen.

For both manufacturing process, fatigue striations were observed (Fig. 14). This is characteristic of transgranular crack propagation mechanism, typically observed in 316L austenitic stainless steel [8].

#### 4. Discussion

Micrographic observations revealed grain refinement, whereas hardness measurements indicated a significant difference between the two manufacturing processes. Several studies [11,12] have identified a relationship between fatigue strength and material hardness. It is generally accepted that resistance to crack initiation in defect-free materials increases with their resistance to plastic deformation. In this regard, the local hardening effect of the flow process should theoretically enhance the material's resistance to

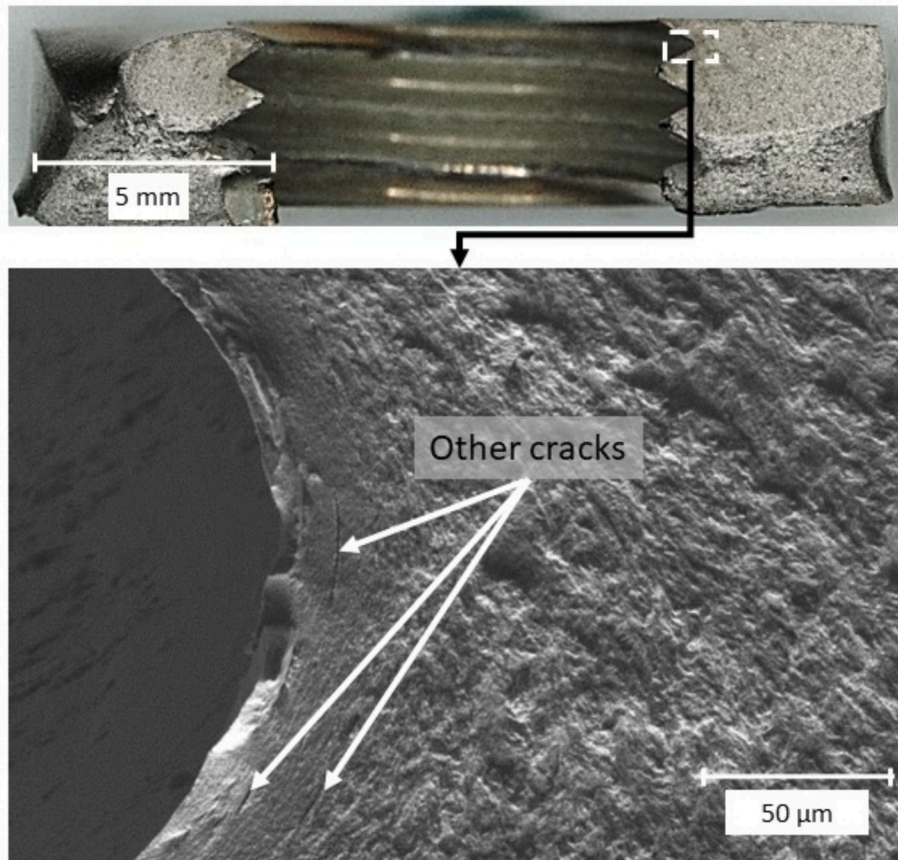


Fig. 13. Cracks in another highly deformed region.

fatigue.

However, the  $M-N$  diagram revealed no significant difference in the fatigue strength values. For the two highest load levels, the average number of cycles to failure was comparable. This phenomenon likely occurred because the surface discontinuities associated with the flow process competed with the positive effect of hardening, resulting in the similar lifespan of C and F specimens.

At lower stress, the flow-formed bars exhibited a 70 % shorter average fatigue life than the machined ones. The most significant difference between the failure of the C and F specimens was the location of the crack initiation site. In the former, cracks initiated at the tip of a thread, whereas for the latter, cracks emerged at the root of a preexisting discontinuity. These discontinuities reduced the number of cycles required to induce crack initiation. Because the proportion of fatigue life spent initiating a crack increased with an overall increase in fatigue life [13], this effect was more significant for the specimens tested at lower force values. Although the material in the thread was hardened, process discontinuities located in that area triggered premature crack initiation, reducing the overall fatigue life of F specimens.

Additionally, the work hardening occurring during the flow tapping is responsible for the grain refinement near the surface of the threads. This was highlighted in Fromentin's thesis [2]. Flow tapping can be likened to shot peening as both are methods of forming by cold deformation. The latter induces compressive residual stresses and significant work hardening. In Maleki et al. study [17], a high rate of work hardening appears to have detrimental effects during fatigue tests. This could also be the case for holes that have undergone flow tapping.

Finally, a chemical etching with 20 % NaOH for 40 s at 3 V revealed the presumed presence of delta ferrite (in blue) and sigma phase (in orange), as shown in Fig. 15. Although this phase is present in the base material, its proportion seems to be higher when the material has undergone flow process. This could be due to the temperatures reached and the kinetics during the flow process. The presence of these phases could weaken the material during four-point bending fatigue tests.

## 5. Conclusion

Despite significant research on improving the fatigue life of stainless-steel implants, the complexity of this problem leaves room for

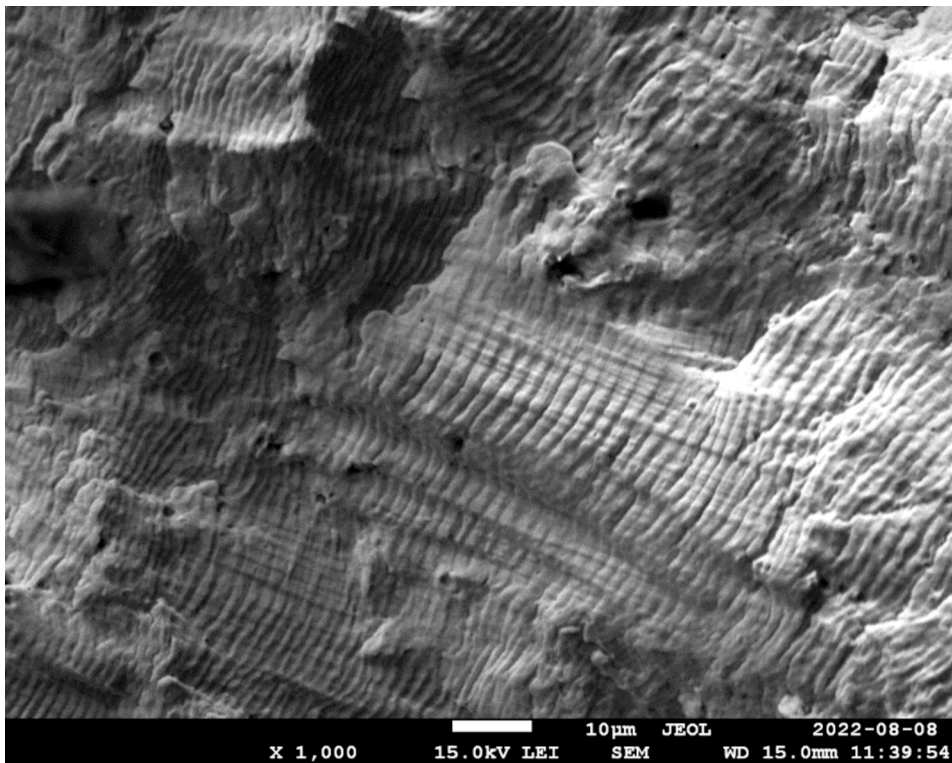


Fig. 14. Fatigue striation observed in a F specimen.

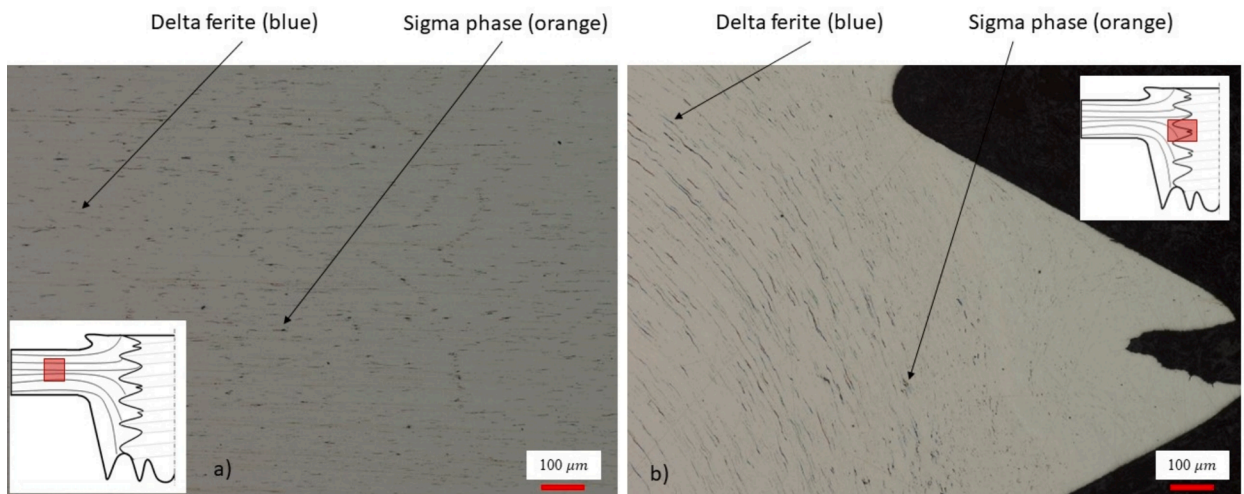


Fig. 15. Phases present in: a) the bulk material and b) a flow processed thread.

further advancements. In this context, this study provided experimental evidence indicating that the successive use of friction drilling and friction tapping did not systematically improve the fatigue life of drilled and tapped plates.

The key observations could be summarized as follows:

1. The flow process induced significant plastic deformation that resulted in a local increase in hardness up to 240 HV. The hardening effect was significant up to 2 mm beneath the threaded surface.
2. Fatigue tests performed with a maximum force greater than 60 % and 75 % of  $F_{\text{yield}}$  indicated comparable fatigue life for the C (drilling and tapping) and F samples.

3. For fatigue tests performed with a maximum force of 50 % of  $F_{\text{yield}}$ , the fatigue life of the F specimens was 70 % shorter than that of the C specimens.
4. In all fatigue tests performed on the F specimens, the crack initiation mechanism was related to the local microstructure features. Cracks initiated at craters and folds created by the flow process. In addition, secondary cracks were observed in the highly deformed regions.

Thus, under the considered conditions, the process of flow drilling followed by flow tapping did not increase the fatigue life of the 316L alloy because of premature crack initiation caused by flow-tapping discontinuities.

Nevertheless, by optimizing the flow process and eliminating discontinuities, this threading process can help improve the fatigue resistance of orthopedic implants. In particular, implants drilled and tapped using a flow process could exhibit superior fatigue life compared with implants subjected to material removal methods. Future studies can be aimed at optimizing flow-forming conditions to limit the formation of discontinuities, thereby enhancing the fatigue strength achievable via work hardening.

### CRediT authorship contribution statement

**Mohamed Akram Mechter:** Writing – review & editing, Writing – original draft, Visualization, Validation, Methodology, Investigation, Formal analysis, Conceptualization. **Mina Gadour:** Writing – original draft, Visualization, Validation, Methodology, Investigation, Formal analysis. **Léa Romain:** Visualization, Investigation. **Oguzhan Tuysuz:** Writing – review & editing. **Myriam Brochu:** Writing – review & editing, Validation, Supervision, Resources, Project administration, Funding acquisition.

### Declaration of competing interest

The authors declare that they have no known competing financial interests or personal relationships that could have appeared to influence the work reported in this paper.

### Data availability

Data will be made available on request.

### Acknowledgments

The authors thank ENS de Rennes (Bruz, France) and SUNI pft (Bruz, France) for fabricating the flow-formed specimens.

### Funding

This work was supported by the Canada Research Chair 2019-00302.

### Appendix A. Supplementary data

Supplementary data to this article can be found online at <https://doi.org/10.1016/j.engfailanal.2024.108730>.

### References

- [1] M. Armentia, M. Abasolo, I. Coria, J. Albizuri, J. Aguirrebeitia, Fatigue performance of prosthetic screws used in dental implant restorations: Rolled versus cut threads, *J. Prosthet. Dent.* 126 (406) (2021) e1–406.e8, <https://doi.org/10.1016/j.prosdent.2021.06.035>.
- [2] G. Fromentin, Mechanical and technological study of the cold form tapping process applied to hardened steel. <https://pastel.hal.science/pastel-00000941>, 2004. Accessed the 03 / 05 / 2024.
- [3] S.F. Miller, P.J. Blau, A.J. Shih, Microstructural alterations associated with friction drilling of steel, aluminum, and titanium, *J. Mater. Eng. Perform.* 14 (2005) 647–653, <https://doi.org/10.1361/105994905X64558>.
- [4] S.F. Miller, J. Tao, A.J. Shih, Friction drilling of cast metals, *Int. J. Mach. Tools Manuf.* 46 (2006) 1526–1535, <https://doi.org/10.1016/j.ijmactools.2005.09.003>.
- [5] H.-M. Chow, S.-M. Lee, L.-D. Yang, Machining characteristic study of friction drilling on AISI 304 stainless steel, *J. Mater. Process Technol.* 207 (2008) 180–186, <https://doi.org/10.1016/j.jmatprotec.2007.12.064>.
- [6] W. Grzesik, B. Kruszynski, A. Ruzaj, *Surface integrity of machined surfaces*, Springer, London, 2010, pp. 143–179.
- [7] J. Maščenik, S. Pavlenko, Effective use of technology flowdrill in production engineering, *Adv. Mat. Res.* 1064 (2014) 171–174, <https://doi.org/10.4028/www.scientific.net/AMR.1064.171>.
- [8] B. Gervais, A. Vadean, M. Raison, M. Brochu, Failure analysis of a 316L stainless steel femoral orthopedic implant, *Case Stud. Eng. Fail Anal.* 5–6 (2006) 30–38, <https://doi.org/10.1016/j.csefa.2015.12.001>.
- [9] S. Mohajerzadeh, K. Farhangdoost, P. Zamani, K. Kolasangiani, Experimental investigation on fatigue evaluation of orthopaedic locking compression plate, *ADMT J.* 11 (2018) 47–52.
- [10] C. Kanchanomai, V. Phiphobmongkol, P. Muanjan, Fatigue failure of an orthopedic implant – A locking compression plate, *Eng. Fail. Anal.* 15 (2008) 521–530, <https://doi.org/10.1016/j.engfailanal.2007.04.001>.

- [11] O. Unal, E. Maleki, I. Karademir, F. Husem, Y. Efe, T. Das, Effects of conventional shot peening, severe shot peening, re-shot peening and precised grinding operations on fatigue performance of AISI 1050 railway axle steel, *Int. J. Fatigue* 155 (2022) 106613, <https://doi.org/10.1016/j.ijfatigue.2021.106613>.
- [12] Y. Zhi, X. Zhang, D. Liu, J. Yang, D. Liu, Y. Guan, J. Shi, W. Zhao, R. Zhao, J. Wu, J. Wang, Improvement of traction-traction fatigue properties of A100 steel plate-hole-structure by double shot peening, *Int. J. Fatigue* 162 (2022) 106925, <https://doi.org/10.1016/j.ijfatigue.2022.106925>.
- [13] K.J. Miller, M.F.E. Ibrahim, Damage accumulation during initiation and short crack growth regimes, *Fatigue Fract Eng. Mater. Struct.* 4 (1981) 2630277, <https://doi.org/10.11011/j.1460-2695.1981.tb01124.x>.
- [14] ASTM E3-11 (2017), Standard Guide for Preparation of Metallographic Specimens <https://www.astm.org/e0003-11r17.html>.
- [15] ASTM E384-22 (2022), Standard test method for microindentation hardness of materials <https://www.astm.org/e0384-22.html>.
- [16] ASTM F382-17 (2017) Standard Specification and Test Method for Metallic Bone Plates <https://www.astm.org/f0382-17.html>.
- [17] E. Maleki, O. Unal, M. Guagliano, S. Bagherifard, Analysing the fatigue behaviour and residual stress relaxation of gradient nano-structured 316l steel subjected to the shot peening via deep learning approach, *Met. Mater. Int.* 28 (1) (2022) 112–131, <https://doi.org/10.1007/s12540-021-00995-8>.